

Electronic Supporting Information

Single Crystalline Ternary Mixed Metal Oxide 1-Dimensional Nanostructures of $\text{Ir}_{1-x-y}\text{Ru}_x\text{V}_y\text{O}_2$ by Vapour Phase Transport

Hayoung Jung^{a†}, Sung Hee Chun^{a†}, Jeesoo Seok^a, Yu Lim Kim^a, Seung Joon Lee^b, Myung Hwa Kim^{a*} and Nam-Suk Lee^{c*}

^a*Department of Chemistry & Nano Science, Ewha Womans University, Seoul, 120-750,
Korea*

^b*Platform Technology Team, Samsung Fine Chemicals R&D Bldg., Suwon, 443-803, Korea*

^c*National Institute for Nanomaterials Technology (NINT), Pohang University of Science and
Technology (POSTECH), Pohang, 790-784, Korea*

[†]*Authors are equally contributed to this work.*

*To whom all correspondence should be addressed: myungkim@ewha.ac.kr,
nslee@postech.ac.kr

Table. S1.

$\text{Ir}_{1-x-y}\text{Ru}_x\text{V}_y\text{O}_2$	XRD	XRD	Calculated	Error (%)
	2θ (degree)	$d(110)$ (\AA)	$d(110)$ (\AA)	
$\text{Ir}_{0.06}\text{Ru}_{0.41}\text{V}_{0.53}\text{O}_2$	27.68	3.223	3.200	0.715
$\text{Ir}_{0.10}\text{Ru}_{0.36}\text{V}_{0.54}\text{O}_2$	27.78	3.211	3.201	0.333
$\text{Ir}_{0.12}\text{Ru}_{0.34}\text{V}_{0.54}\text{O}_2$	27.76	3.214	3.202	0.366
$\text{Ir}_{0.14}\text{Ru}_{0.74}\text{V}_{0.12}\text{O}_2$	28.18	3.167	3.182	0.493
$\text{Ir}_{0.23}\text{Ru}_{0.34}\text{V}_{0.43}\text{O}_2$	27.78	3.211	3.197	0.446
$\text{Ir}_{0.39}\text{Ru}_{0.37}\text{V}_{0.24}\text{O}_2$	28.00	3.187	3.190	0.113
$\text{Ir}_{0.40}\text{Ru}_{0.44}\text{V}_{0.16}\text{O}_2$	28.10	3.175	3.187	0.353

* $d(110)$ for IrO_2 : 3.186 \AA , $d(110)$ for RuO_2 : 3.176 \AA , $d(110)$ for VO_2 : 3.220 \AA

* Copper X-ray Wavelength : 1.5418 pm

Table. S1. The d -spacing values for the crystallographic planes of (110) of various compositions of $\text{Ir}_{1-x-y}\text{Ru}_x\text{V}_y\text{O}_2$ ternary mixed metal oxide nanowires from XRD measurements and estimated ones with reference data from JCPDS.

Fig. S1

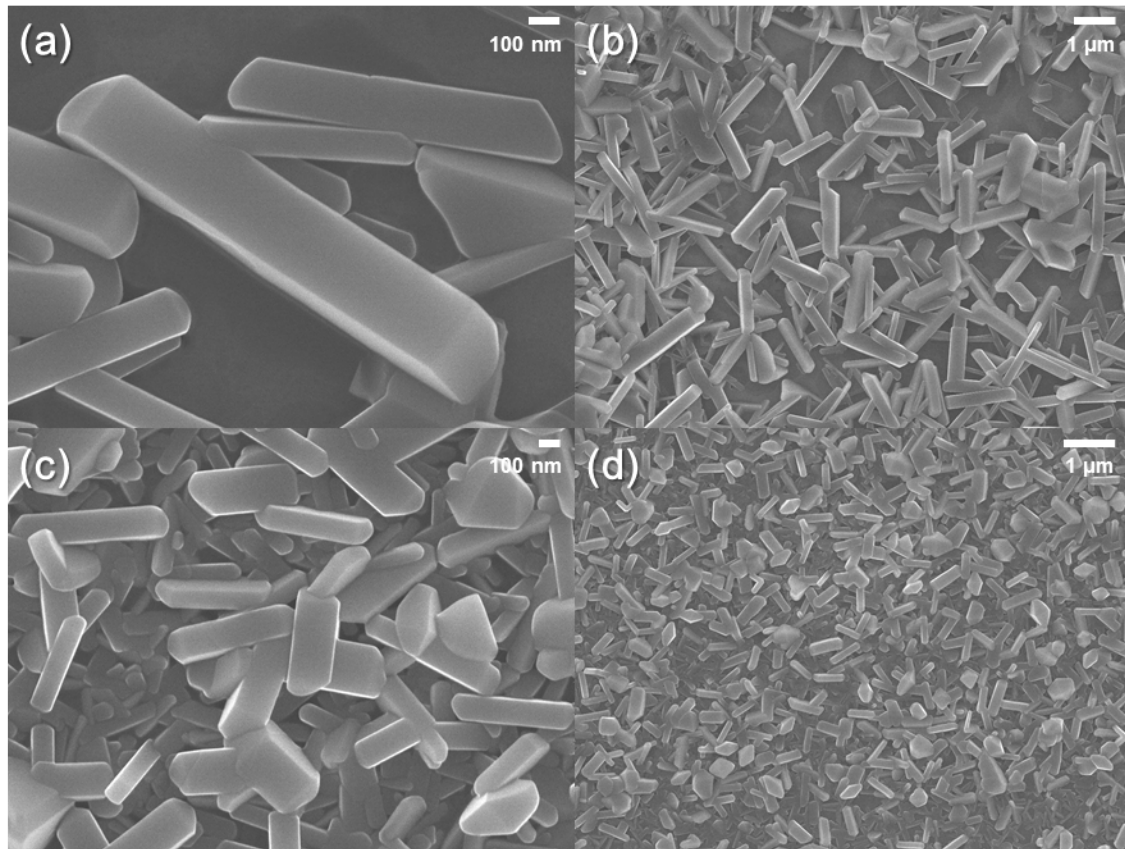


Fig. S1 SEM images of as-grown iridium-ruthenium-vanadium ternary mixed metal oxide nanowires on a Si(001) substrate by a vapour transport process. (a) and (b) $\text{Ir}_{0.06}\text{Ru}_{0.41}\text{V}_{0.53}\text{O}_2$, (c) and (d) $\text{Ir}_{0.10}\text{Ru}_{0.36}\text{V}_{0.54}\text{O}_2$.

Fig. S2.

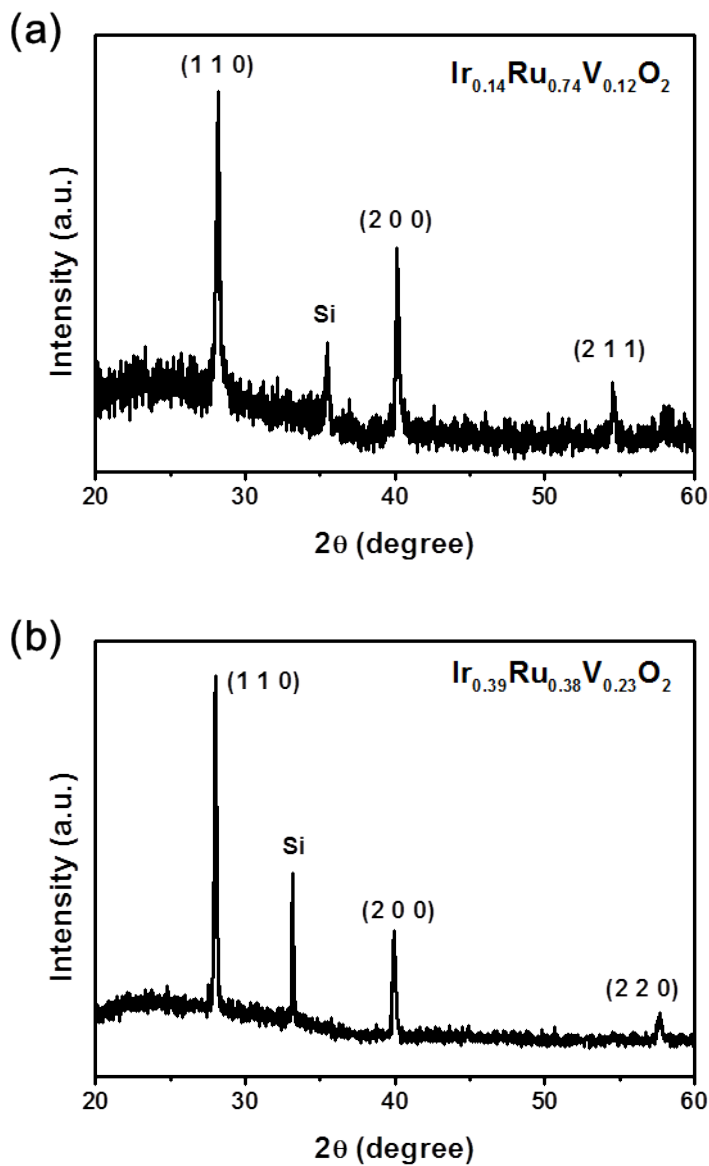


Fig. S2. XRD patterns of $\text{Ir}_{1-x-y}\text{Ru}_x\text{V}_y\text{O}_2$ ternary mixed metal oxide nanowires at a variety of compositions.

Fig. S3.

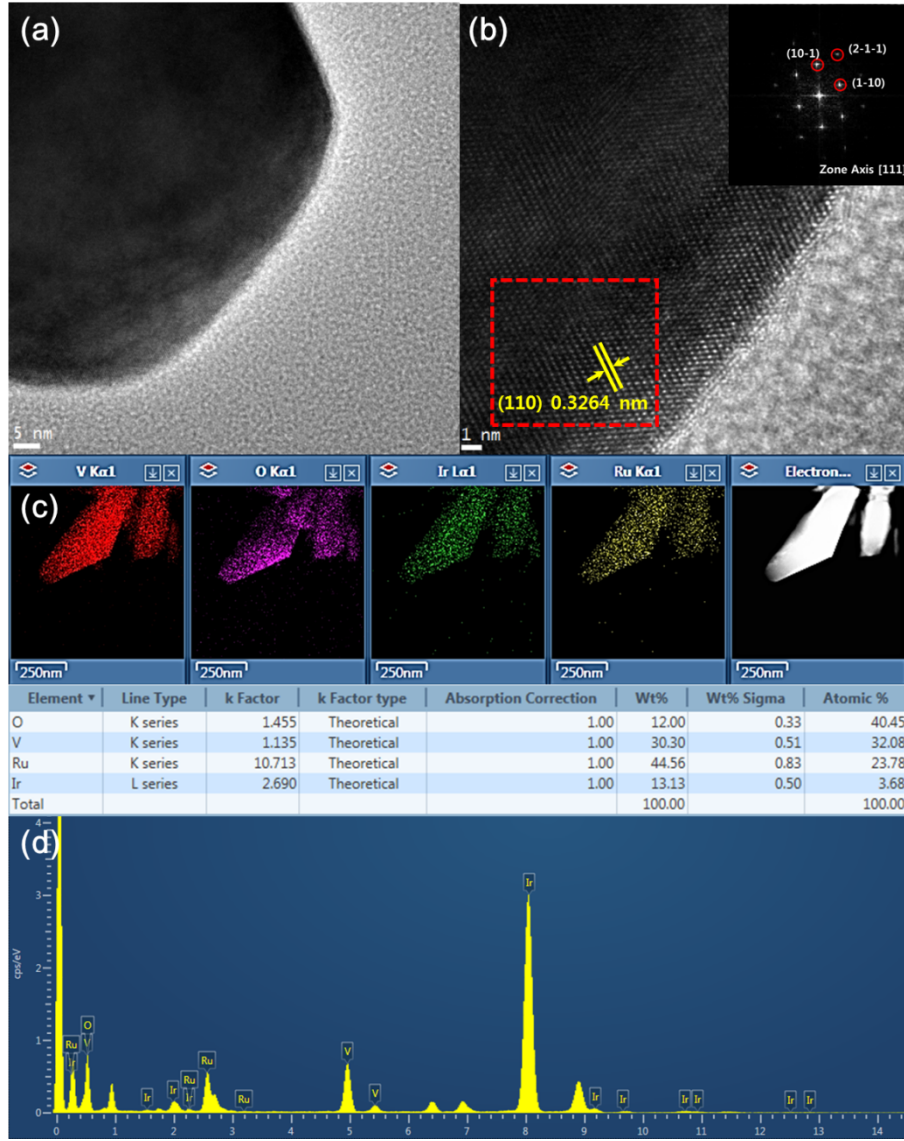


Fig. S3. (a) The low magnification TEM images and (b) the lattice resolved HRTEM image of a single $\text{Ir}_{0.06}\text{Ru}_{0.41}\text{V}_{0.53}\text{O}_2$ ternary mixed metal oxide nanowire. (c) EDS-elemental mapping analysis for Ir(L), Ru(K) and V(K) atoms and (d) EDS spectrum of a single $\text{Ir}_{0.06}\text{Ru}_{0.41}\text{V}_{0.53}\text{O}_2$ ternary mixed metal oxide nanowire.

Fig. S4.

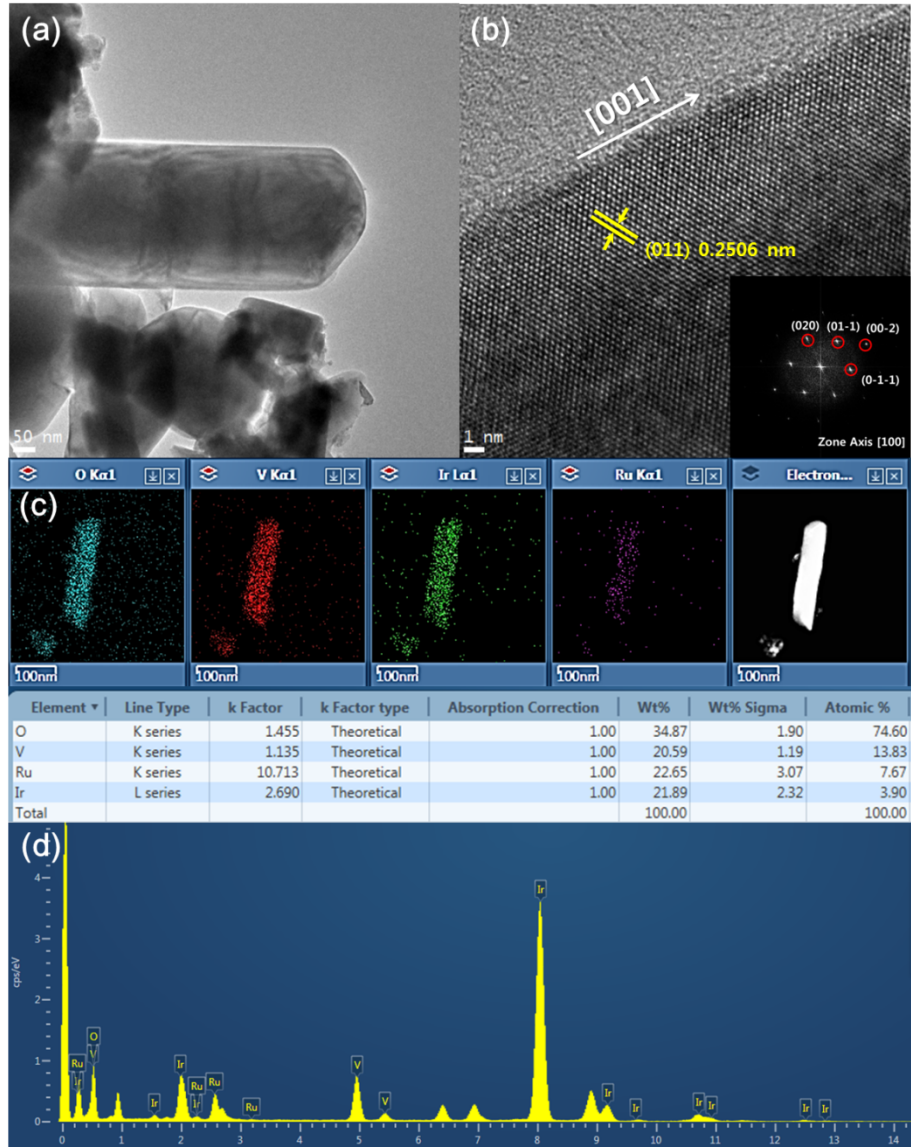


Fig. S4. (a) The low magnification TEM images and (b) the lattice resolved HRTEM image of a single $\text{Ir}_{0.10}\text{Ru}_{0.36}\text{V}_{0.54}\text{O}_2$ ternary mixed metal oxide nanowire. (c) EDS-elemental mapping analysis for Ir(L), Ru(K) and V(K) atoms and (d) EDS spectrum of a single $\text{Ir}_{0.10}\text{Ru}_{0.36}\text{V}_{0.54}\text{O}_2$ ternary mixed metal oxide nanowire.

Fig. S5.

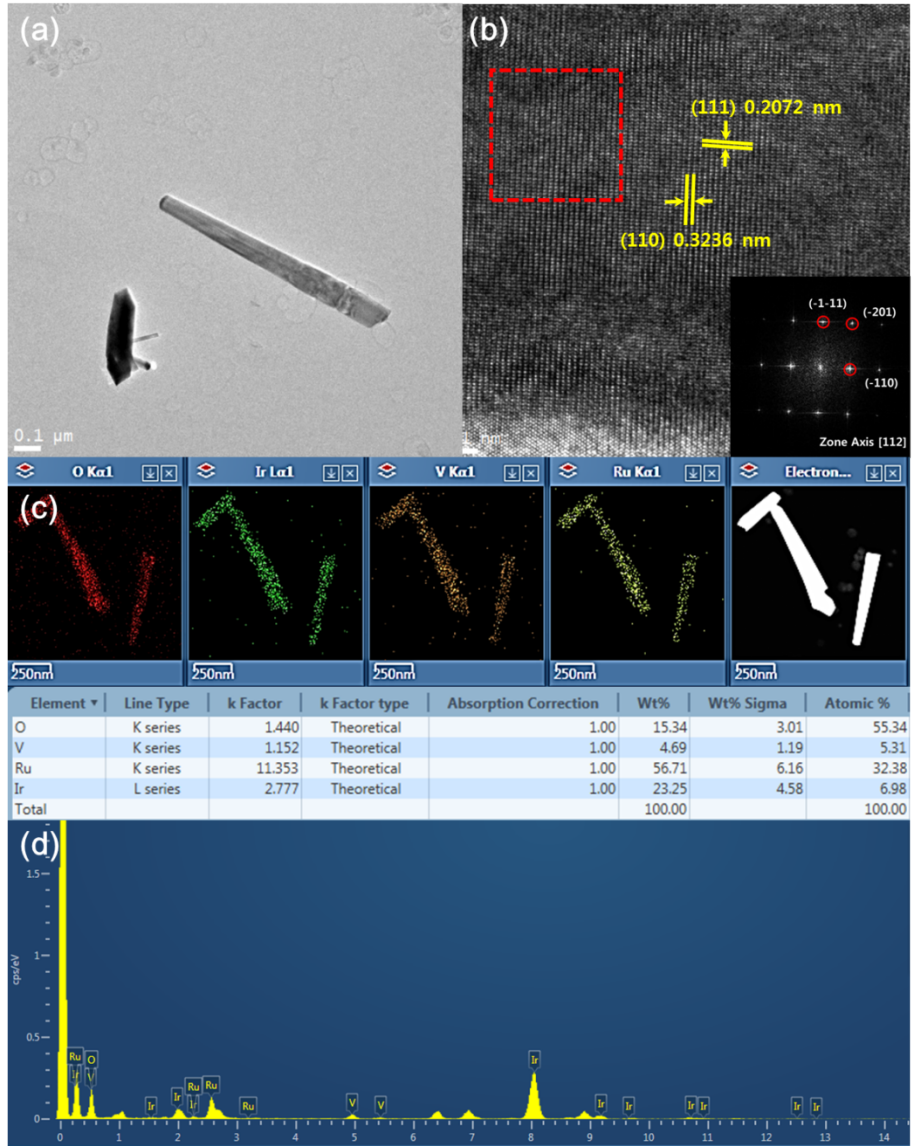


Fig. S5. (a) The low magnification TEM images and (b) the lattice resolved HRTEM image of a single $\text{Ir}_{0.14}\text{Ru}_{0.74}\text{V}_{0.12}\text{O}_2$ ternary mixed metal oxide nanowire. (c) EDS-elemental mapping analysis for Ir(L), Ru(K) and V(K) atoms and (d) EDS spectrum of a single $\text{Ir}_{0.14}\text{Ru}_{0.74}\text{V}_{0.12}\text{O}_2$ ternary mixed metal oxide nanowire.

Fig. S6.

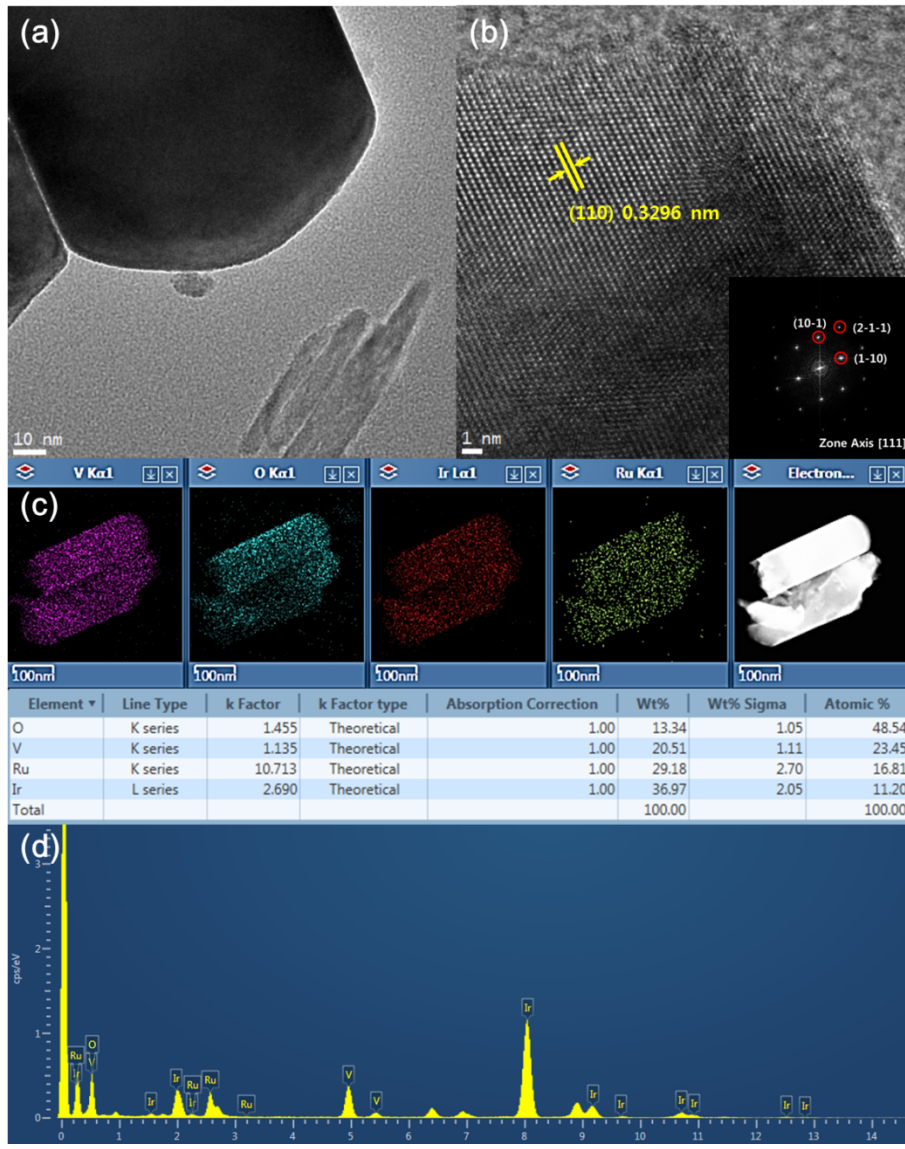


Fig. S6. (a) The low magnification TEM images and (b) the lattice resolved HRTEM image of a single $\text{Ir}_{0.23}\text{Ru}_{0.34}\text{V}_{0.43}\text{O}_2$ ternary mixed metal oxide nanowire. (c) EDS-elemental mapping analysis for Ir(L), Ru(K) and V(K) atoms and (d) EDS spectrum of a single $\text{Ir}_{0.23}\text{Ru}_{0.34}\text{V}_{0.43}\text{O}_2$ ternary mixed metal oxide nanowire.

Fig. S7.

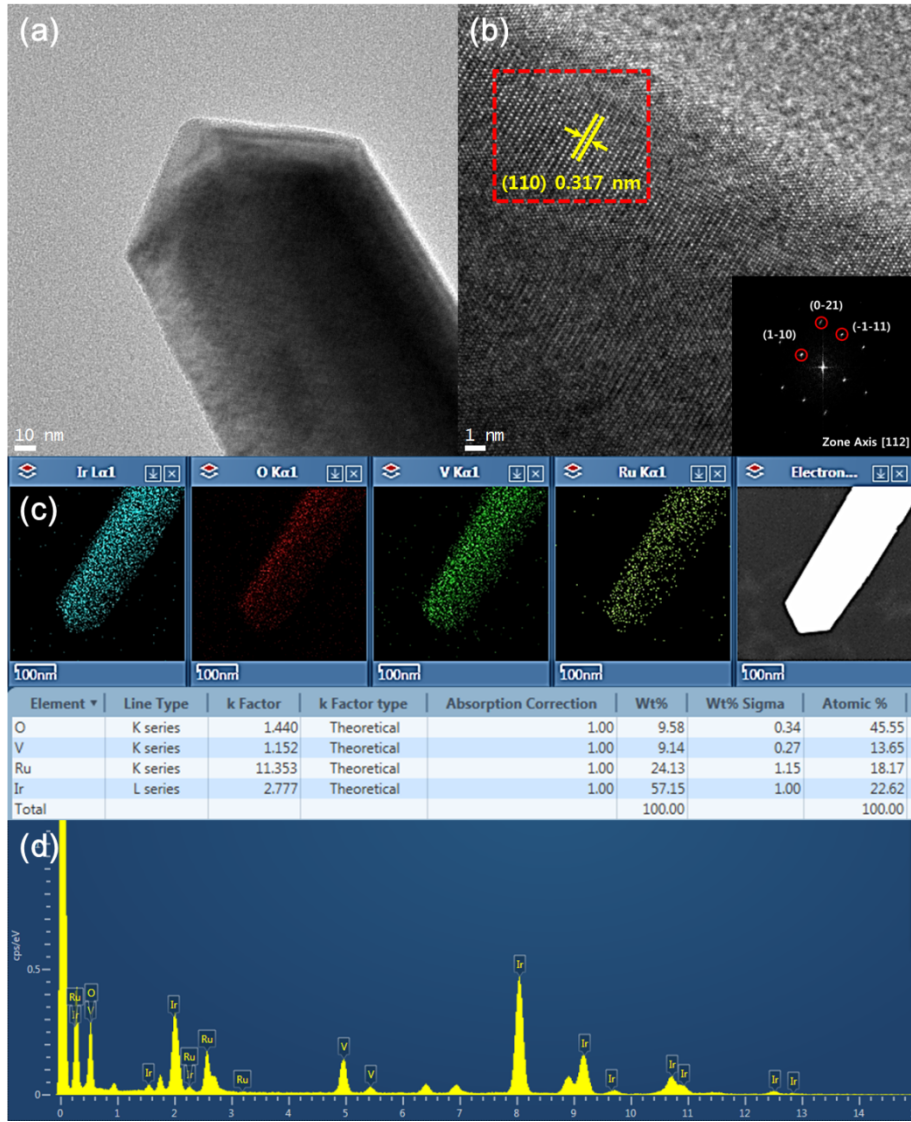


Fig. S7. (a) The low magnification TEM images and (b) the lattice resolved HRTEM image of a single $\text{Ir}_{0.39}\text{Ru}_{0.37}\text{V}_{0.24}\text{O}_2$ ternary mixed metal oxide nanowire. (c) EDS-elemental mapping analysis for Ir(L), Ru(K) and V(K) atoms and (d) EDS spectrum of a single $\text{Ir}_{0.39}\text{Ru}_{0.37}\text{V}_{0.24}\text{O}_2$ ternary mixed metal oxide nanowire.

Fig. S8.

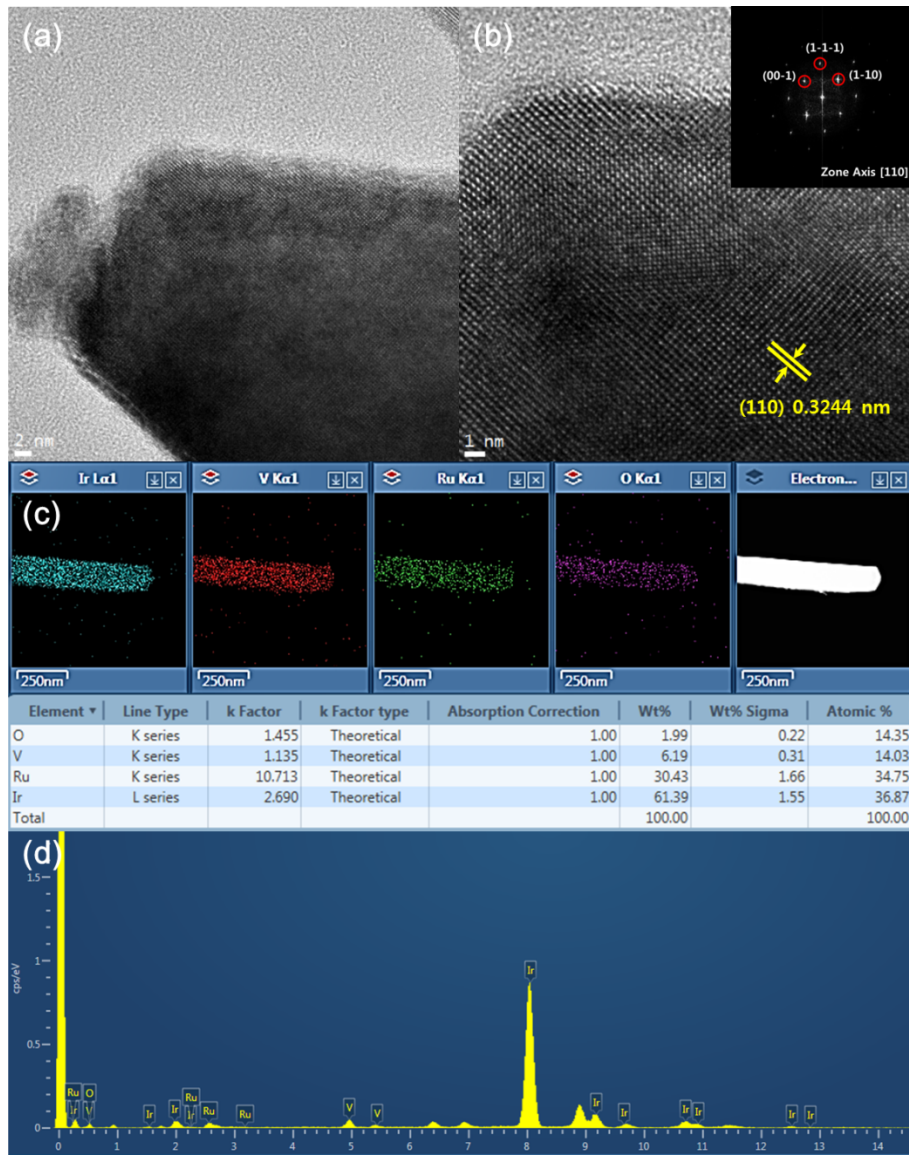


Fig. S8. (a) The low magnification TEM images and (b) the lattice resolved HRTEM image of a single $\text{Ir}_{0.40}\text{Ru}_{0.44}\text{V}_{0.16}\text{O}_2$ ternary mixed metal oxide nanowire. (c) EDS-elemental mapping analysis for Ir(L), Ru(K) and V(K) atoms and (d) EDS spectrum of a single $\text{Ir}_{0.40}\text{Ru}_{0.44}\text{V}_{0.16}\text{O}_2$ ternary mixed metal oxide nanowire.

Fig. S9.

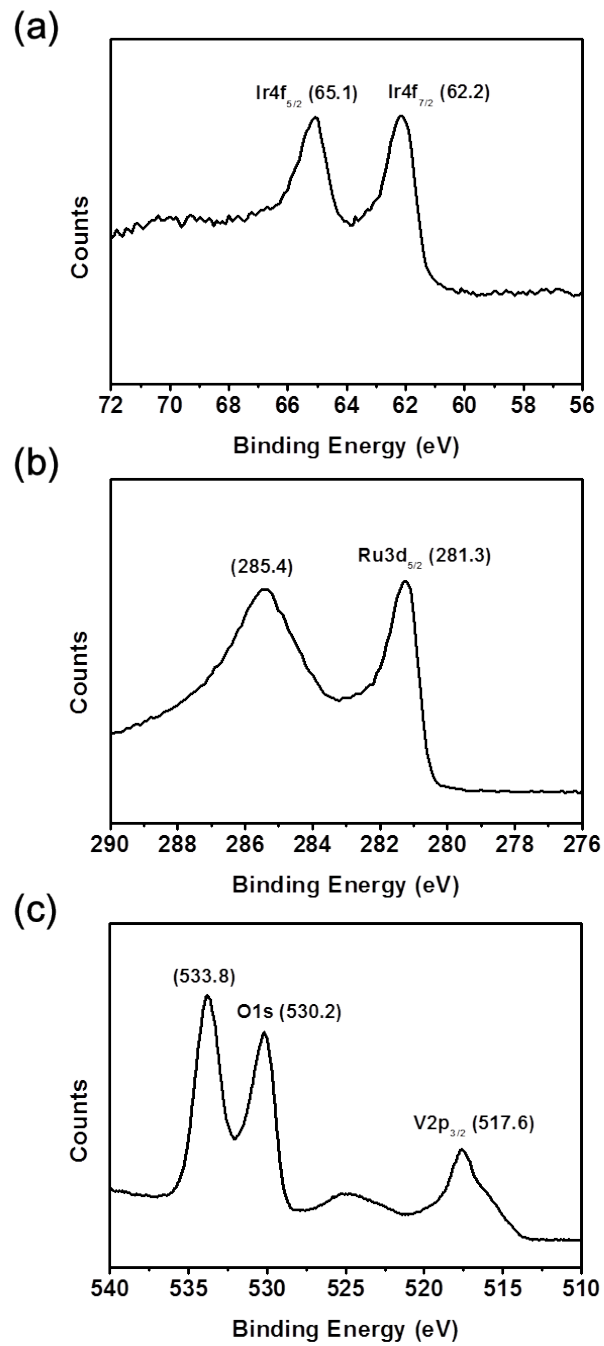


Fig. S9. X-ray Photoelectron Spectroscopy (XPS) data of $\text{Ir}_{0.06}\text{Ru}_{0.41}\text{V}_{0.53}\text{O}_2$ mixed metal oxide nanowires for (a) Ir 4f, (b) Ru 3d, and (c) V 2p.

Fig. S10.

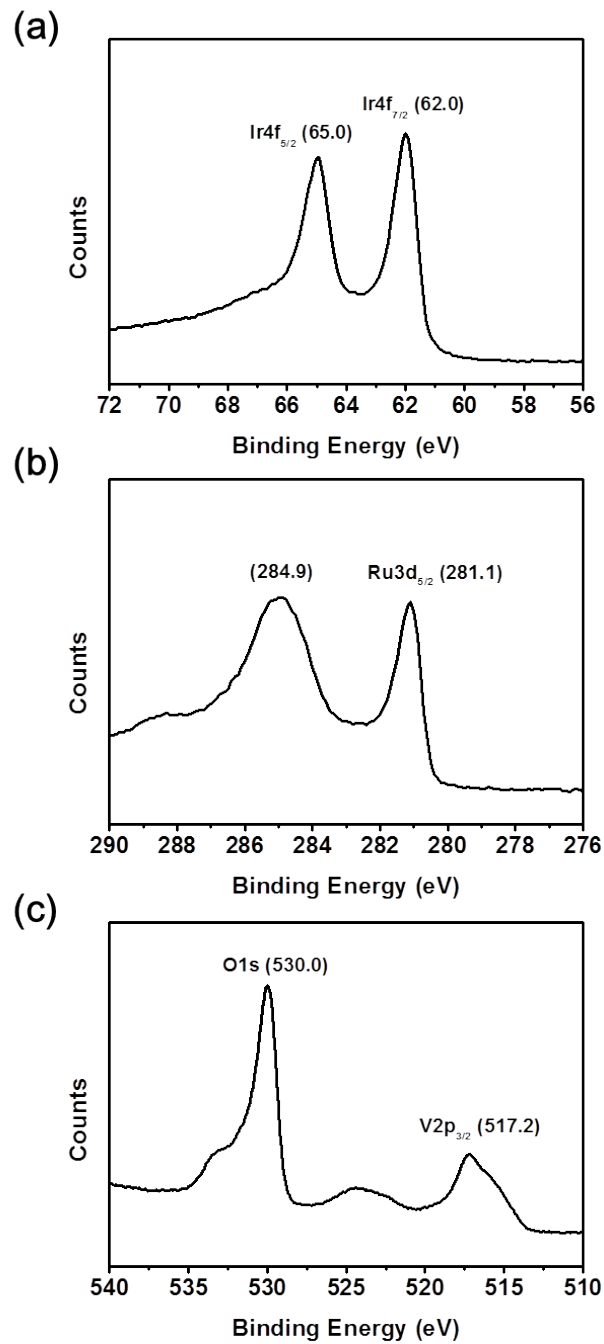


Fig. S10. X-ray Photoelectron Spectroscopy (XPS) data of Ir_{0.10}Ru_{0.36}V_{0.54}O₂ mixed metal oxide nanowires for (a) Ir 4f, (b) Ru 3d, and (c) V 2p.

Fig. S11.

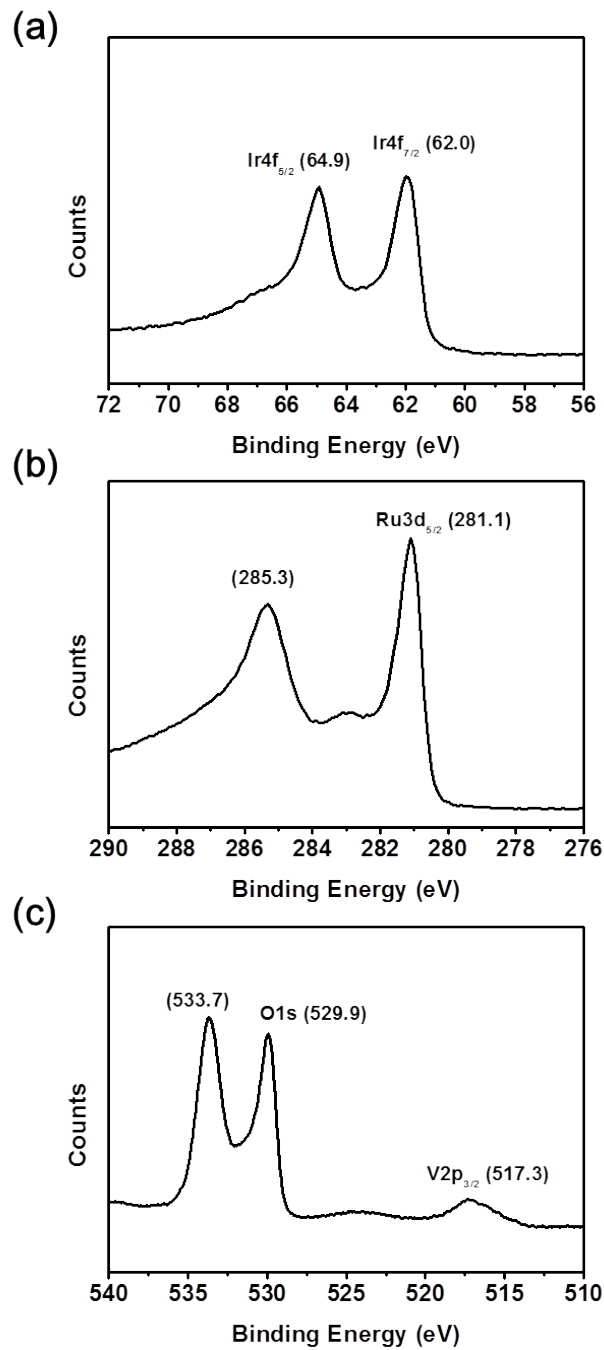


Fig. S11. X-ray Photoelectron Spectroscopy (XPS) data of $\text{Ir}_{0.14}\text{Ru}_{0.74}\text{V}_{0.12}\text{O}_2$ mixed metal oxide nanowires for (a) Ir 4f, (b) Ru 3d, and (c) V 2p.

Fig. S12.

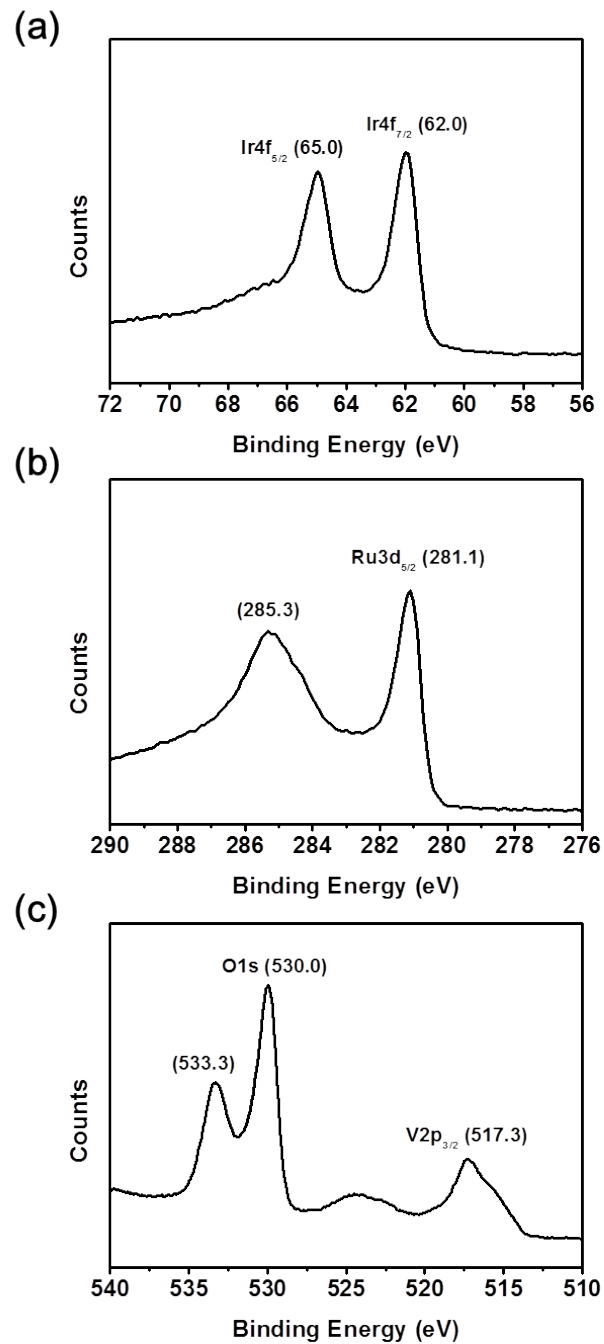


Fig. S12. X-ray Photoelectron Spectroscopy (XPS) data of $\text{Ir}_{0.23}\text{Ru}_{0.34}\text{V}_{0.43}\text{O}_2$ mixed metal oxide nanowires for (a) Ir 4f, (b) Ru 3d, and (c) V 2p.

Fig. S13.

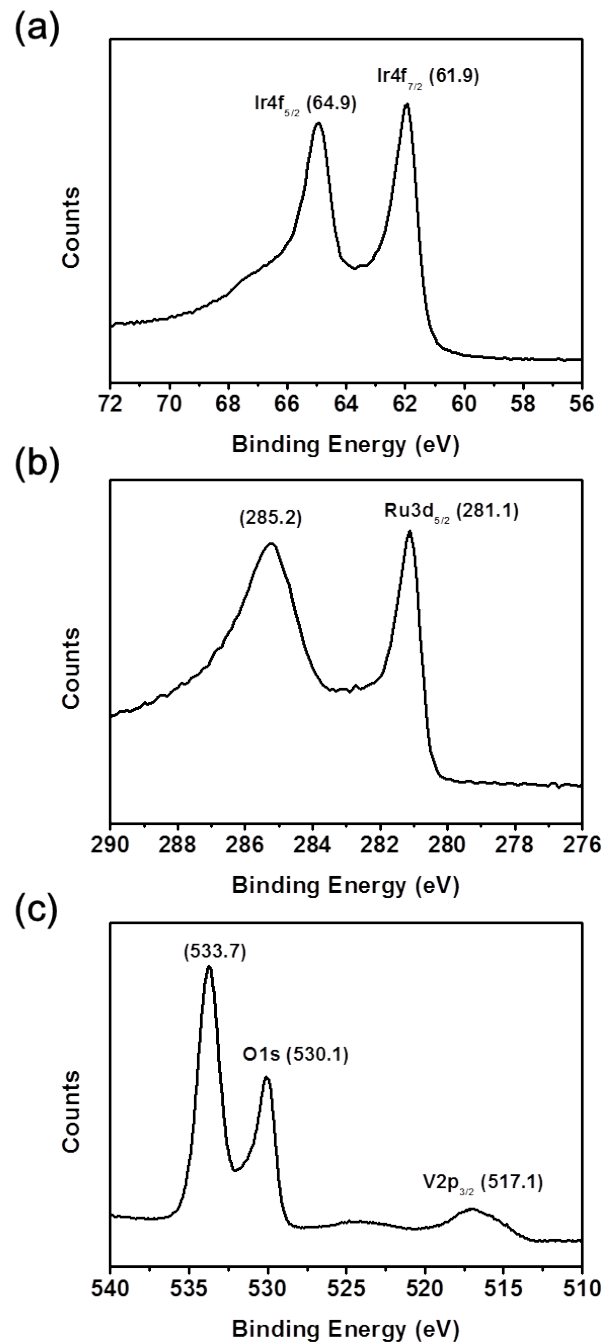


Fig. S13. X-ray Photoelectron Spectroscopy (XPS) data of $\text{Ir}_{0.39}\text{Ru}_{0.37}\text{V}_{0.24}\text{O}_2$ mixed metal oxide nanowires for (a) Ir 4f, (b) Ru 3d, and (c) V 2p.